Carrier phase estimation scheme for faster-than-Nyquist optical coherent communication systems

Chengcheng Li (李程程)[1], Dongwei Pan (潘董威)[1], Yiqiao Feng (冯一乔)[1], Jiachuan Lin (林嘉川)[1], Lixia Xi (席丽霞)[1], Xianfeng Tang (唐先锋)[1], Wenbo Zhang (张文博)[2], and Xiaoguang Zhang (张晓光)[1,*]

[1]*State Key Laboratory of Information Photonics and Optical Communications, Beijing University of Posts and Telecommunications, Beijing 100876, China*

[2]*School of Science, Beijing University of Posts and Telecommunications, Beijing 100876, China*

**Corresponding author: xgzhang@bupt.edu.cn*

Received May 8, 2016; accepted August 5, 2016; posted online August 30, 2016

We propose a modified-Viterbi and Viterbi phase estimation (VVPE) carrier phase recovery scheme that shows an effective capability of reducing the frequent and accumulated cycle slips induced by inter-symbol interference (ISI) in a faster-than-Nyquist (FTN) optical coherent communications system. In a 28-Gbaud FTN polarization-division multiplexed quadrature phase-shift keying optical communication system, the comparison of the proposed modified-VVPE scheme and the conventional VVPE scheme is carried out. It is proved that the proposed modified-VVPE scheme can effectively overcome the challenge of ISI induced error carrier phase estimation, which leads to a better bit error ratio performance.

OCIS codes: 060.1660, 060.2330, 060.4510.
doi: 10.3788/COL201614.100601.

The rapid growth in internet applications leads to the ever-increasing demand for higher spectral efficiency in optical transmission systems. Spectral efficiency can be increased by advanced modulation formats like quadrature phase-shift keying (QPSK), 16-quadrature amplitude modulation (16QAM), or reducing of channel spacing. Advanced modulation formats are widely used because they can increase spectral efficiency by several times, but they need a higher optical signal-to-noise ratio (OSNR), which limits the transmission distance[1–5]. Recently, faster-than-Nyquist (FTN) signaling has attracted much attention because this technology can compress the occupation bandwidth to a fraction of the bandwidth that the Nyquist signal occupies[6–9]. Meanwhile, in an FTN system the symbol period between two adjacent pulses is lower than that of the corresponding Nyquist system, with the result that inter-symbol interference (ISI) is introduced[10–13]. Fortunately, we can use a detection method such as the maximum *a posteriori* (MAP) or maximum likelihood sequence estimation (MLSE) to overcome this challenge on the coherent receiver side[12–16].

With the recent advancement of high-speed digital signal processing (DSP), DSP-based methods have been introduced for high-speed optical systems and have achieved great success. Carrier phase recovery (CPR) is the important part of the DSP process, whose function is to remove the phase noise (PN) induced by the transmitter (Tx) laser and the local oscillator (LO) at the receiver (Rx) end. Many CPR algorithms have been proposed such as the Viterbi and Viterbi phase estimation (VVPE) algorithm, blind phase search (BPS) algorithm, and pilot-assisted–carrier phase recovery (PA–CPR) scheme[17–19]. Among them, the VVPE algorithm has a low complexity but a not so good performance. The BPS algorithm has the best performance, but the complexity is the highest. These two methods cannot work well in the FTN system because of ISI induced by FTN signaling, showing a large possibility of a new kind of accumulated cycle slips that will degrade the correcdt estimation of PN. This situation becomes worse especially in the systems with larger linewidth of the Tx and LO lasers and severe ISI due to denser compression of bandwidth by FTN. In our previous work, a PA–CPR scheme is proposed[20] that can overcome the effect of ISI introduced by an FTN system, with the sacrifice of a redundant bandwidth, which is contrary to the goal to save bandwidth by using an FTN system[21].

In this work, we propose a modified-VVPE algorithm that is proved to have good performance in an FTN system. The model of the PN caused by lasers in an FTN system is analyzed. The basic principles of the modified-VVPE scheme are presented. Optimization of the main parameters like the sliding window length, are also investigated to get an optimum performance of the proposed algorithm. We find that the modified-VVPE can correctly track the PN in spite of severe ISI when the bandwidth is sufficiently compressed by the FTN technique. The comparison of the proposed algorithm with the traditional VVPE scheme is carried out in a 28-Gbaud FTN–PDM–QPSK optical communication system. The results show that with a 1 dB OSNR penalty at the BER of 1.0×10^{-2} (threshold value of the soft-decision forward error correction), the proposed algorithm demonstrates the good performance with a lower BER, lower cycle slips ratio (CSR), and the high tolerance to the laser linewidth.

The concept of FTN was first proposed by Mazo in 1975[7]; the signal pulses were accelerated and became faster than the Nyquist signal pulses by $1/\tau$ ($\tau < 1$ is a compression factor). The key change of the FTN signal from the Nyquist signal is that the sequential FTN signal symbols are no longer orthogonal each other. Assuming the symbol period is τT, the FTN signal sequence can be written as

$$S(t) = \sqrt{E_s}\sum_n a_n h(t - n\tau T), \tag{1}$$

where a_n is independent complex-valued symbols, each pulse has energy E_s, and $h(t)$ is the shape of the signal pulse. If a filter matched to $h(t)$ is used in the detection, its samples at $n\tau T$ will contain ISI as well.

In this work, we mainly focus on the influence of ISI on laser PN estimation and assume all liner optical impairments have been precompensated, and only amplified spontaneous emission (ASE) noise induced by EDFAs (erbium-doped fiber amplifiers) will be considered. So the model of the received signal can be described as

$$r(t) = [x(t) + \mathrm{ISI}]\, e^{j\theta(t)} + n(t), \tag{2}$$

where $\theta(t)$ is the PN caused by the laser linewidth and $n(t)$ represents a zero-mean white Gaussian noise with a variance of σ_n^2. $x_k = \sqrt{2}e^{j\phi_k}$ involves the QPSK modulated information with $\phi(t) = (2k+1)\frac{\pi}{4}$, $k = (1,2,3,4)$ and $\mathrm{ISI} = \sigma(t)e^{j\varphi(t)}$ is caused by time domain compression. Then the input symbol entering the CPR module can be expressed as

$$\begin{aligned} r_k &= (x_k + \mathrm{ISI})\, e^{j\theta_k} + n_k, \\ &= \left(\sqrt{2}e^{j\phi_k} + \sigma_k e^{j\varphi_k}\right) e^{j\theta_k} + n_k, \\ &= \left(\sqrt{2} + \sigma_k'\right) e^{j(\phi_k + \varphi_k')} \cdot e^{j\theta_k} + n_k, \end{aligned} \tag{3}$$

where σ_k' and φ_k' are the amplitude noise and PN, respectively, caused by ISI for the FTN system. After CPR, Bahl–Cocke–Jelinek–Raviv (BCJR) or a Viterbi algorithm (VA) detector is used to detect the signal and eliminate ISI, whose process belongs to the MAP or MLSE detection. When we use the traditional VVPE algorithm to recover the phase, the signal can be expressed as

$$\begin{aligned} r_k^4 &= \left[\left(\sqrt{2} + \sigma_k'\right) e^{j(\phi_k + \varphi_k')} \cdot e^{j\theta_k} + n_k\right]^4, \\ &= \left(\sqrt{2} + \sigma_k'\right)^4 e^{j4(\theta_k + \varphi_k')} \cdot e^{j4\phi_k} + n_k', \\ &= -\left(\sqrt{2} + \sigma_k'\right)^4 e^{j4(\theta_k + \varphi_k')} + n_k', \end{aligned} \tag{4}$$

where n_k' includea the cross terms and n_k^4. PN $\theta_k + \varphi_k'$ takes the place of θ_k. Obviously, additional interference of φ_k' due to ISI will make traditional VVPE fail in phase tracking, as shown in Fig. 1.

By a large number of simulation experiments, we find that the main consequence of φ_k' in the process of phase tracking is more frequent occurrence of a new kind of cycle slips, as shown Fig. 1 (for example, positions A, B, C ..... in Fig. 1). Unlike the sharp slip between the symbols before and after occurring in ordinary coherent detection systems, the cycle slips due to ISI in an FTN system behave as accumulated and cover several symbols (see inset of Fig. 1). The larger scale of ISI happens more frequently for this kind of accumulated cycle slips. Therefore, we can come to the conclusion that, without any improvement, traditional VVPE would face the challenge of the new kind of cycle slips when intentional ISI is severe. So, in this work, we do some work to improve the performance of the VVPE algorithm.

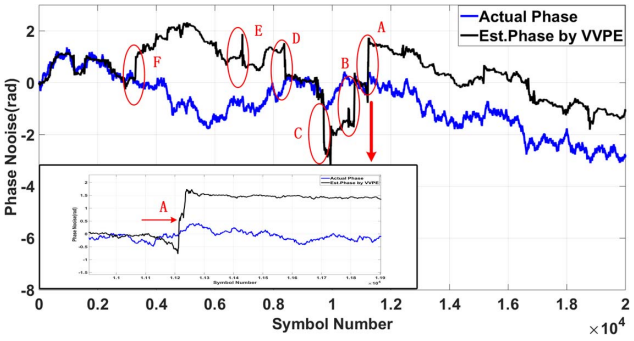

Fig. 1. PN tracking performances of VVPE in the case of $\tau = 0.75$.

In order to solve the problem of these kind of accumulated cycle slips and get the correct estimation of PN in the PDM–QPSK FTN system, we take further action after the VVPE algorithm. The modified-VVPE frame is shown in Fig. 2. First, the signal is performed by fourth power, addition, and taking phase angle actions that are the same as the traditional VVPE scheme. After that, another sliding window (not the sliding window used in conventional VVPE that locates at the Σ module in Fig. 2) is used to solve the accumulated cycle slips. The sliding window covers every $2m+1$ symbols to evaluate the accumulated cycle slip as

$$\Delta_k = \left\lfloor \frac{\varphi(k+m) - \varphi(k-m)}{\frac{\pi}{2}} \right\rfloor \times \frac{\pi}{2}, \tag{5}$$

where $\varphi(k+m)$ and $\varphi(k-m)$ are the phases of the first and the last signals covered in the sliding window. When the Δ_k is larger than a given optimized threshold (here m and threshold should be optimized in advance), we can conclude that there is an accumulated cycle slip here. Then the compensation of cycle slip is carried out. The mathematical formula is shown as

$$\varphi(k+m) = \varphi(k-m) - \Delta_k. \tag{6}$$

In this way, we can obtain a correct CPR. Then, the BCJR or VA detector is used to solve the rest of the problems due to ISI for the FTN system.

Figure 3 shows the system setup for the proposed modified-VVPE scheme in the polarization-division

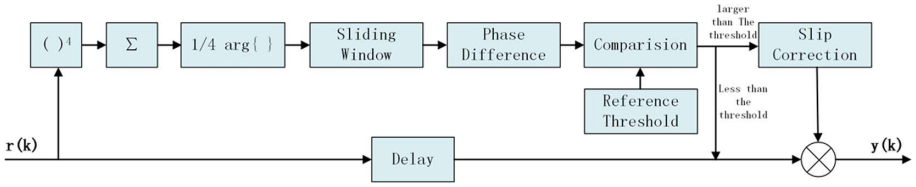

Fig. 2. Logic diagram of the modified-VVPE algorithm.

multiplexing (PDM)–QPSK FTN transmission system. The binary sequence is coded and mapped to the QPSK FTN signal. Then, the carrier signal is modulated by an IQ modulator driven by the FTN-pulse-shaped QPSK signal at the symbol rate of 28 Gbaud. The X and Y branches of the FTN signal are coupled together by a polarization beam coupler, then the dual-polarization states of the optical signal are generated.

At the Rx side, a coherent front end with a LO is used to provide a treatment of the electrical signal corresponding to the I and Q components for both polarization states. The central frequency of the LO is the same as the central frequency of the signal carrier. The hybrid is used within the coherent receivers to superposition the signal light and the LO light. Then the I and Q signals $I_I(t)$ and $I_Q(t)$ are sampled by A/D converters (ADCs). After the ADC, these signals are processed in the DSP unit. In the simulation, we mainly focus on signals' CPR, so we assume that the linear noises such as chromatic dispersion (CD) and polarization mode dispersion (PMD) have been compensated completely. Afterward, the signals with PN are compensated by the proposed modified-VVPE algorithm, and the MLSE symbol detector based on the VA is used to detect signals. Finally, the BER is calculated in order to evaluate the performance of the proposed algorithm.

System simulations are implemented utilizing the simulation software of MATLAB. We first give the optimization of significant parameters that can guarantee the best performance of the proposed modified-VVPE scheme. In the simulation, we consider PDM–QPSK modulation format with a baud rate of 28 Gbaud, which corresponds to a bit rate of 112 Gb/s. The laser PN is modeled as a Winer process[17]. In addition, we load different amounts of ASE noise to obtain different levels of OSNR, which is defined as the optical signal-to-noise power ratio with a 0.1 nm reference bandwidth.

The sliding window (located at the Σ module in Fig. 2) length N is an important parameter that has a great influence on the performance of the system. Then, we measure the relation between the CSR and the linewidth duration product $\Delta f \cdot T_s$ with the different N, as shown in Fig. 4. The signal compression ratio of the FTN system is set to be 0.75 and the OSNR is 10 dB. The results show that the optimal N is 200 at the small linewidth region (several hundred kilohertz (kHz)) and is 150 at the large linewidth region (several megahertz (MHz)) for the traditional VVPE algorithm, the optimal N is 150 at the small linewidth region, and is 80 at the large linewidth region for the modified-VVPE algorithm. It is easy to account for that because, when the PN is small, the ASE noise is larger with respect to PN, and we need a larger length to wipe out the ASE noise. On the contrary, when the PN is larger with respect to the ASE noise, we need to decrease the length to track the variation of PN. Hence, the optimum value of the sliding window length is necessary to guarantee the performance of the CPR scheme.

In order to assess the performance of our proposed modified-VVPE algorithm, we track the actual PN by using the VVPE scheme and the modified-VVPE algorithm when the OSNR is 12 dB, the compression factor is 0.75, and the linewidth duration product $\Delta f \cdot T_s$ is chosen to be 3×10^{-5} in the PDM–QPSK FTN system, as shown in Fig. 5. The result shows that the modified-VVPE algorithm can track the phase fluctuation successfully, while the VVPE scheme cannot track the PN accurately because of the accumulated cycle slips. Therefore, the modified-VVPE algorithm can overcome the challenge of the accumulated cycle slip induced by ISI in despite of the larger linewidth.

Then the CSR of the VVPE and the modified-VVPE algorithm is analyzed with the optimal parameter N in

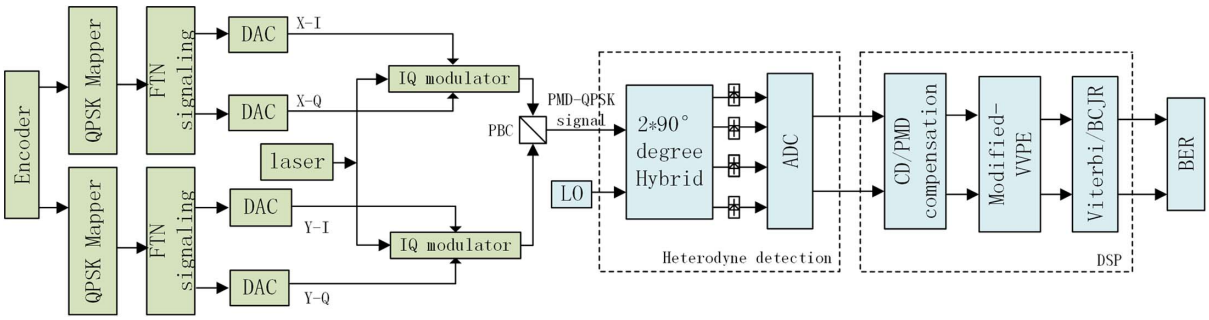

Fig. 3. Architecture of the PDM–QPSK FTN transmission system.

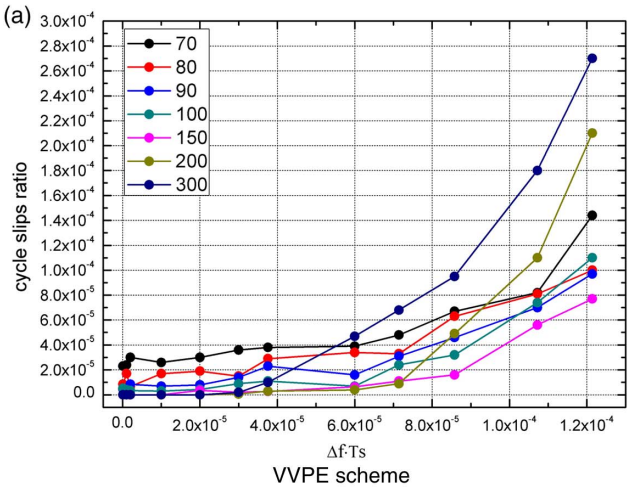

Fig. 4. Linewidth symbol duration product versus CSR with different block lengths: (a) VVPE scheme, (b) modified-VVPE scheme.

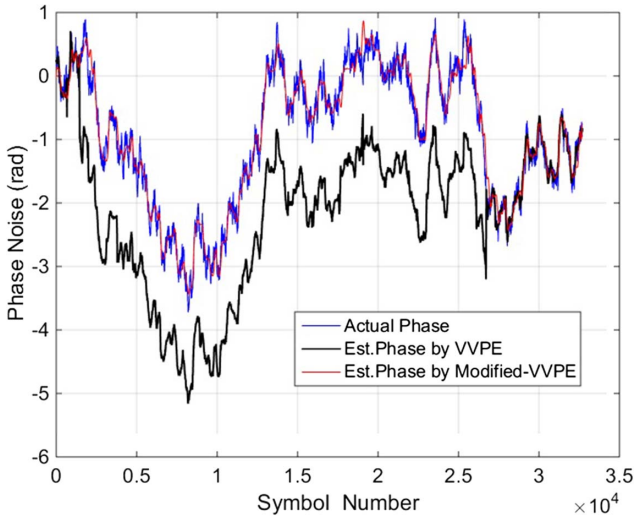

Fig. 5. PN tracking performances of the VVPE and the modified-VVPE.

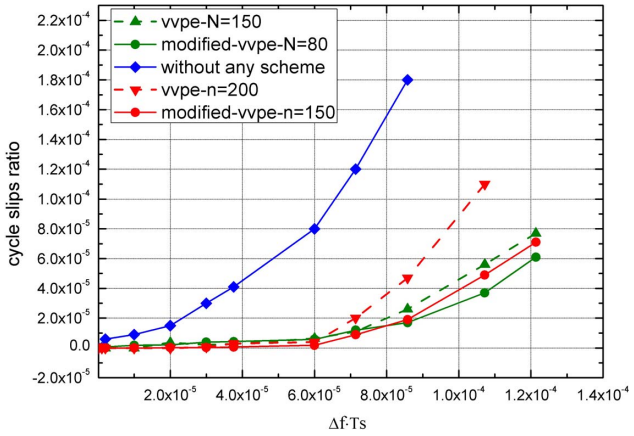

Fig. 6. CSR of the VVPE and modified-VVPE algorithm.

the PDM–QPSK FTN system. As shown in Fig. 6, the CSR is very high without any recovery algorithm; the CSR using the modified-VVPE algorithm is smaller than the VVPE algorithm with the optimal parameter N.

As a further study, we make the comparison of the BER performances using the VVPE scheme and the

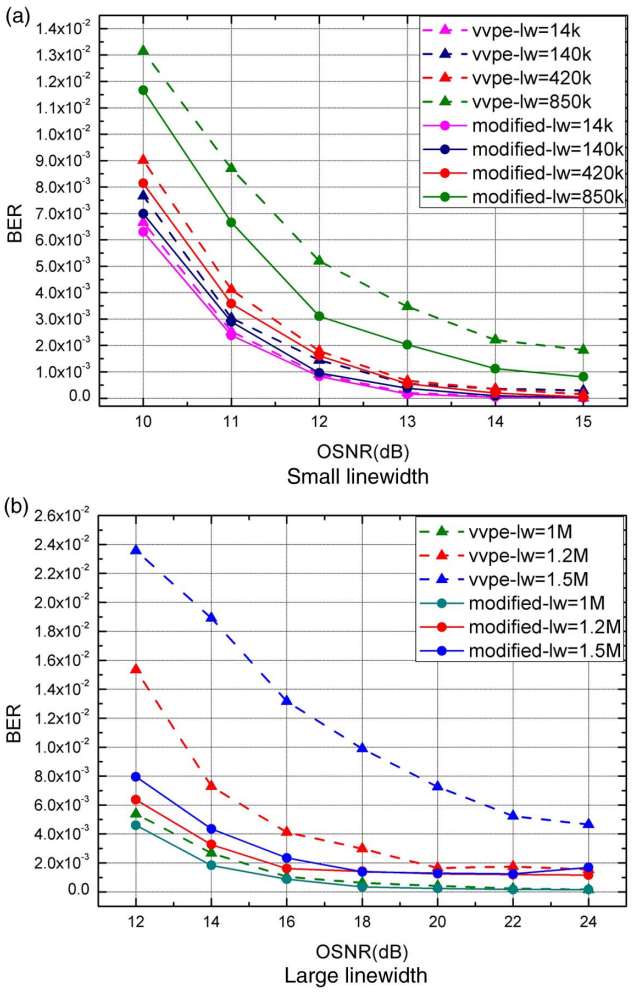

Fig. 7. BER versus OSNR performance at different linewidths: (a) amall linewidth and (b) large linewidth.

modified-VVPE algorithm in the PDM–QPSK FTN system under the different OSNRs with the different linewidths in both small and large linewidth regions. The modified-VVPE algorithm behaves better than the VVPE scheme with the same linewidth, especially better in large linewidth region, as shown in Fig. 7(a) and 7(b). Therefore, the modified-VVPE algorithm can overcome the challenge of ISI in despite of the larger scale of laser linewidth.

Figure 8 depicts the OSNR penalty versus $\Delta f \cdot T_s$ at a BER of 1.0×10^{-2} (threshold value of soft-decision forward error correction). The case with a zero hertz linewidth without using any CPR algorithms is regarded as the reference for penalty calculation. In Fig. 8, we can find that the modified-VVPE scheme shows low OSNR penalty requirements both in the small laser linewidth region and the large laser linewidth region. It turns out that the modified-VVPE scheme outperforms the VVPE scheme. On the right side of Fig. 8 the constellation diagrams of the received FTN signal and the recovered signal are also presented.

At the BER of 1.0×10^{-2}, the linewidth tolerance value of $\Delta f \cdot T_s$ at 1 dB OSNR penalty is defined as the maximum tolerable value $(\Delta f \cdot T_s)_{\max}$. Table 1 gives $(\Delta f \cdot T_s)_{\max}$ for different schemes and the sliding window length and the corresponding linewidth tolerance values $\Delta v_{\max}$ at 28 Gbaud. We can conclude that the modified-VVPE scheme shows a good linewidth tolerance performance in the PDM–QPSK FTN system.

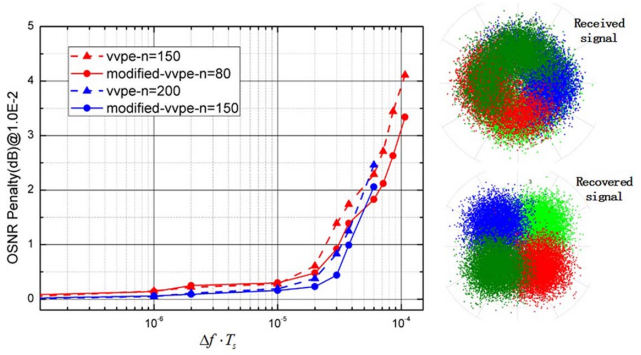

Fig. 8. OSNR penalty vs. different values of $\Delta f \cdot T_s$ at BER $= 1.0 \times 10^{-2}$.

Table 1. Linewidth Tolerance of Various Length N for VVPE and Modified-VVPE in a PDM–QPSK FTN System

Length N	$(\Delta f \cdot T_s)_{\max}$	$\Delta v_{\max}$ at 28 Gbaud (MHz)
150 (VVPE)	2.5×10^{-5}	0.700
80 (M-VVPE)	3.1×10^{-5}	0.868
200 (VVPE)	3.3×10^{-5}	0.924
150 (M-VVPE)	3.9×10^{-5}	1.092

In conclusion, we present a modified-VVPE algorithm as the CPR scheme in a 28 Gbaud PDM–QPSK FTN system. We give the mathematical model of the signal in the system and the principle of the proposed modified-VVPE algorithm. Optimization of the sliding window length N in the scheme is studied for different laser linewidths. Finally, a comparison of the performances of the modified-VVPE algorithm and the VVPE scheme is conducted in terms of CSR, BER, and laser linewidth tolerance. It turns out that the modified-VVPE algorithm has a lower CSR, lower BER, and higher laser linewidth tolerance, which behaves better than the traditional VVPE scheme.

This work was supported by the National Natural Science Foundation of China (Nos. 61571057, 61527820, and 61575082) and the Open Fund of the Guangdong Provincial Key Laboratory of Optical Fiber Sensing and Communications (Jinan University).

References

1. M. Seimetz, *High-order Modulation for Optical Fiber Transmission* (Springer, 2009).
2. E. Ip, A. P. T. Lau, D. J. F. Barros, and J. M. Kahn, Opt. Express **16**, 753 (2008).
3. X. Zhou, IEEE Signal Process. Mag. **31**, 35 (2014).
4. K. Kikuchi, in *European Conference on Optical Communication*, 1 (2008).
5. C. Li, M. Luo, X. Xiao, J. Li, Z. He, Q. Yang, Z. Yang, and S. Yu, Chin. Opt. Lett. **12**, 040601 (2014).
6. D. Dasalukunte, V. Owall, F. Rusek, and J. B. Anderson, *Faster than Nyquist Signaling* (Springer, 2014).
7. J. E. Mazo, Bell Labs Tech. J. **54**, 1451 (1975).
8. G. Colavolpe, T. Foggi, A. Modenini, and A. Piemontese, Opt. Express **19**, 26600 (2011).
9. L. Li, Y. Lu, L. Liu, D. Chang, Z. Xiao, and Y. Wei, in *Optical Fiber Communication Conference*, W3J-2P (2014).
10. K. Wang, Y. Lu, and L. Liu, in *Optical Fiber Communication Conference*, W3E-2 (2015).
11. J. B. Anderson, F. Rusek, and V. Wall, Proc. IEEE **101**, 1817 (2013).
12. M. Secondini, T. Foggi, F. Fresi, G. Meloni, F. Cavaliere, G. Colavolpe, E. Forestieri, L. Potí, R. Sabella, and G. Prati, J. Lightwave Technol **33**, 3558 (2015).
13. A. Barbieri, D. Fertonani, and G. Colavolpe, IEEE Trans. Comms. **57**, 2951 (2009).
14. B. M. Hochwald and S. T. Brink, IEEE Trans. Comms. **51**, 389 (2003).
15. S. Hu and F. Rusek, arXiv preprint arXiv, 07331 (2015).
16. T. Pfau, S. Hoffmann, and R. Noé, J. Lightwave Technol. **27**, 989 (2009).
17. X. Su, L. Xi, X. Tang, Z. Zhang, S. Bai, W. Zhang, and X. Zhang, IEEE Photon. Tech. Lett. **27**, 77 (2015).
18. X. Zhou, K. Zhong, Y. Gao, C. Lu, A. P. T. Lau, and K. Long, Opt. Express **22**, 24044 (2014).
19. W. Zhang, D. Pan, X. Su, X. Zhang, L. Xi, and X. Tang, Chin. Opt. Lett. **14**, 020601 (2014).
20. D. Pan, X. Tang, Y. Feng, C. Li, J. Lin, L. Xi, W. Zhang, and X. Zhang, Opt. Fiber Technol. **26**, 135 (2015).
21. H. Cheng, Y. Li, D. Kong, J. Zang, J. Wu, and J. Lin, Opt. Express **22**, 20740 (2014).